

# Shaped Pattern Synthesis for Equispaced Linear Arrays with Non-Isotropic Antennas

T.M. Brintjes, A.B.J. Kokkeler, G. Karagiannis and G.J.M. Smit

Department of Electrical Engineering, Mathematics and Computer Science, University of Twente

P.O. Box 217, 7500AE Enschede, The Netherlands

email: t.m.brintjes@utwente.nl

**Abstract**—This paper explains how the measured directivity of antenna elements can be taken into account during shaped pattern synthesis. The method that is presented is based on the Orchard Elliott synthesis procedure. Important features of this classical way of synthesizing shaped antenna patterns are its high degree of control over the pattern's shape, and the flexible way in which the array excitations can be chosen. However, because it operates on the array factor, the directivity (i.e., element factor) of the antenna elements is neglected. Once synthesis is complete, and the element factor is reintroduced to evaluate the actual beam pattern, one often finds that the overall shape is not as it was specified. In particular when the shaped region of the pattern is placed further away from broadside, the differences become substantial. In those cases it may be necessary to take the element factor into account during synthesis.

**Keywords**—Shaped pattern synthesis, antenna directivity, element factor.

## I. INTRODUCTION

Within the field of shaped (null-free) pattern synthesis, one could make a differentiation between the classic analytical methods and the more recent numerical techniques. Analytical methods, which started with Woodward [1], take a direct approach while numerical techniques mostly formulate the synthesis problem such that it is suitable for (global) optimization. Simulated Annealing[2], Genetic Algorithms [3], Particle Swarm Optimization [4] or other techniques [5][6] can then be used to solve it. Numerical synthesis of shaped beam patterns is very generic. Difficulties such as arbitrary array geometries, differently oriented antenna elements and also the directivity of the individual elements can easily be taken into account. Analytical methods are much more limited. However, when the positioning and orientation of the antenna elements is sufficiently regular (e.g., equispaced linear arrays), an analytical approach often provides more precise control over the pattern's shape.

In an earlier publication [7], the analytical approach invented by Orchard et al [8] was chosen to synthesize shaped beam patterns for tracking purposes. This method will be referred to as Orchard Elliott synthesis. The main reasons for choosing Orchard Elliott synthesis are its ability to produce a very smooth ripple in the shaped region, and the fact that it uses the Schelkunoff unit circle representation [9]. Schelkunoff's representation is advantageous because it provides the designer a number of options to choose the beam pattern's array excitations conveniently [10]. The low ripple makes it possible to estimate the direction of arrival (DoA) based on the power received from an asymmetrically (ramp) shaped beam pattern [7]. When the DoA can be determined from the power output

only, mobile wireless devices can be tracked efficiently (i.e., without the need for scanning) using a single output (fully) analog beamformer. However, it was found that the shape of the pattern is affected to an unacceptable degree by the non-isotropic gain of the array elements. This is in particular problematic for shaped patterns outside the *broadside* [11] region, which has led to the investigation of how the element factor can be incorporated in the synthesis algorithm.

In [12] it has been suggested that Orchard Elliott synthesis can be applied to non-isotropic antenna elements, however, without further elaborating on this. Our paper details exactly how to incorporate the (measured) directivity of physical antennas in the Orchard Elliott synthesis method. Section II first introduces the problem of synthesizing beam patterns and in particular how Orchard and Elliott approached it. The most relevant steps of their synthesis method are emphasized after which the modifications necessary for element factor compensation are explained in Section III. As an example, the synthesis of a ramp shaped pattern is shown in Section IV, followed by some practical hints for computational stability in section V and a discussion in Section VI. Conclusions based on synthesizing various commonly used shaped patterns are drawn in Section VII.

## II. ANALYSIS

Under the assumption that all antenna elements are identical and oriented in the same direction [11], the beam pattern  $B(\theta)$  of an equispaced linear antenna array can be separated into an *array factor*  $AF(\theta)$  and an *element factor*  $EF(\theta)$ :

$$B(\theta) = AF(\theta)EF(\theta) \quad (1)$$

The element factor corresponds to the gain of the antennas and the array factor of an  $N$ -element array is given by:

$$AF_{\theta}(\theta) = \sum_{n=0}^{N-1} I_n e^{jn \frac{2\pi d}{\lambda} \sin(\theta)}, \quad (2)$$

where  $I_n$  is the excitation (also known as coefficient or weight) of the  $n^{\text{th}}$  element,  $d$  the spacing between the elements and  $\theta$  the angle of incidence with respect to the array normal. When a spacing of  $d = 1/2\lambda$  is assumed, the array factor is periodic with a  $180^\circ$  period. This period is also known as the array's *visible region* [11].

For analytical reasons, the simplification  $EF = 1$  (i.e., assuming the isotropic antenna model) is commonly applied to replace (1) by (2). Substituting  $\psi = \frac{2\pi d}{\lambda} \sin(\theta)$  then yields:

$$AF_\psi(\psi) = \sum_{n=0}^{N-1} I_n e^{jn\psi}, \quad (3)$$

which is an expression for the array factor in terms of the frequency independent variable  $\psi$ . A second substitution  $w = e^{j\psi}$ , followed by factorization gives:

$$AF_w(w) = I_N \prod_{n=1}^{N-1} (w - w_n), \quad (4)$$

where  $I_N$  is usually chosen 1 for convenience, and in which the variable  $w$  lies on the Schelkunoff unit circle [9]. When a root  $w_n$  of this polynomial also lies on the unit circle, it can be recognized as a *null* at angle  $\arg(w_n)$  in the array factor. However, if the root is positioned off the unit circle ( $|w_n| \neq 1$ ), the corresponding null will be ‘filled’ [10]. Furthermore, a *lobe* between two nulls is lowered when the distance between the roots is decreased and raised when the distance is increased [13]. A combination of the two enables the creation of (null-free) shaped regions.

The synthesis procedure by Orchard et al [8] essentially displaces the roots of (4) systematically until its shape sufficiently approximates a specified contour  $S$ . In order to control the shape effectively, the roots are decomposed to  $w_n = e^{a_n + jb_n}$  and (4) is rewritten to:

$$\begin{aligned} G(\psi) &= 10\log_{10}(AF_\psi^2(\psi)) \\ &= \sum_{n=1}^{N-2} 10\log_{10}[1 - 2e^{a_n} \cos(\psi - b_n) + e^{2a_n}] \\ &\quad + 10\log_{10}[2(1 + \cos(\psi))] + C, \end{aligned} \quad (5)$$

which is the (power) pattern expressed in dB. The constant  $C$  is used to normalize the power to a convenient reference level (e.g., 0 dB). Fig. 1 shows  $G(\psi)$  for  $N = 16$ . The roots  $w_n$  of this pattern are uniformly distributed around the unit circle:

$$a_n = 0 \quad (6)$$

$$b_n = \pm \frac{2n}{N} \pi \cup -\pi \quad (n = 1, 2, \dots, N/2 - 1) \quad (7)$$

which is the same as using uniform excitations in (3). Note that the term outside the summation in (5) fixes the position of one root at  $w_n = -1$  (i.e., the circled null at  $-\pi$  in Fig. 1), preventing simultaneous angular root displacement [13]. The particular location  $-\pi$  is preferred because it constrains the other roots to be within the visible region ( $\psi = -\pi \dots \pi$ ).

The desired pattern shape is specified in a shaping contour  $S(\psi)$ . Typically part of  $S(\psi)$  describes a region with null filling (region I) and another part (region II) where a certain side lobe topography is specified. A ramp shaped region I, used in [7] for DoA estimation, with uniform side lobe suppression of  $-30$  dB (Fig. 1) serves as an example throughout this paper. Let there be  $N_1$  roots located in region I and  $N_2$  roots in region II. This gives in total  $N_1 + N_2 + 1 = N - 1$  roots, including the one fixed at  $w_n = -1$ . For the shape of the pattern it does not matter whether a region I root is outside the unit circle ( $|w_n| > 1$ ) or inside ( $|w_n| < 1$ ) [10]. This creates  $2^{N_1}$  possible

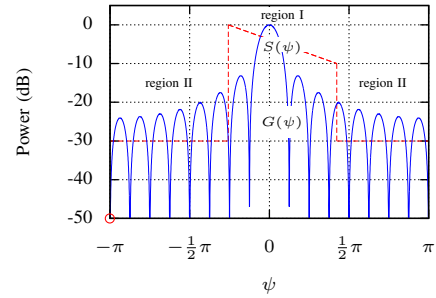


Fig. 1. Array factor  $G(\psi)$  for  $N = 16$  and the desired shape  $S(\psi)$ .

combinations of root, which can be exploited to optimize the array excitations  $I_n$  found by expanding (4).

Starting from a suitable initial pattern, the synthesis procedure iteratively perturbs  $a_n$  and  $b_n$  simultaneously to find better root positions to approximate  $S(\psi)$ . For this paper, the relevant steps of one such iteration are finding the local maxima of  $G(\psi)$  in region II and finding the minima and maxima of the ripple created by  $G(\psi) - S(\psi)$  in region I. Following the Orchard Elliott approach, these values are derived from (5) but in this paper the objective is to obtain them from a function  $GE(\psi)$ , in which the element factor  $E(\psi)$  has been incorporated.

### III. INCORPORATING THE ELEMENT FACTOR

#### A. Initial pattern and shape specification

Almost any pattern can serve as a starting point, as long as it leads to well defined minima and maxima for region I ( $a_n \neq 0$ ). The pattern proposed in the original work of Orchard et al [8]:

$$a_n = \begin{cases} 0.1, & \text{in region I} \\ 0, & \text{in region II} \end{cases} \quad (8)$$

$$b_n = \left( \frac{2n}{N+1} - 1 \right) \pi \quad (n = 2, 3, \dots, N) \quad (9)$$

positions the main lobe adjacent to  $-\pi$ , which ensures that the location of the shaped region remains fairly stable during synthesis. The power pattern resulting from these roots is illustrated for  $N = 16$  by the thick line in Fig. 2.

Let region I be specified between two arbitrarily chosen angles  $\psi_0$  and  $\psi_1$  ( $\psi_1 > \psi_0$ ), and the location of the main lobe's peak be denoted by  $\psi_m$  (Fig. 2). Because  $S(\psi)$  must be specified relative to  $\psi_m$ , it is necessary to shift the desired shaping contour by  $\delta\psi = \psi_m - \psi_0$ :

$$S'(\psi) = S(\psi - \delta\psi) \quad (10)$$

Once the pattern has converged on  $S'(\psi)$ , region I and II will have the desired shape but not the desired location. By rotating *all* roots  $-\delta\psi$  around the unit circle *simultaneously* (i.e.,  $b_n = b_n - \delta\psi$ ), region I can be brought back to the originally specified location  $\psi_0 \dots \psi_1$ . When the element factor is uniform over all  $\psi$ , this process will not affect the shape of the pattern, as shown by the thin line in Fig. 2.

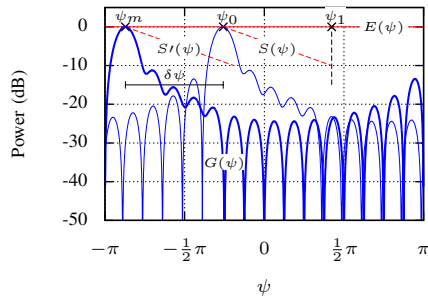


Fig. 2. Beam pattern (shifted) using isotropic antennas.

### B. The element factor

Incorporating the element factor in (5) requires that it is characterized first. Most likely, this characterization will be a set of measurements rather than a closed form expression. Let the set of measurements be denoted by  $\mathbf{E}$ . Throughout this paper, the gain of a customly designed 10 GHz wideband antenna, measured every  $3^\circ$  in the far field (Fig. 3), is used as the element factor. This antenna is currently used in an experimental optical beam steering setup [14], which is envisioned to use shaped beam patterns for tracking [7]. Note that only the measurements between  $-90^\circ$  and  $90^\circ$  around boresight are relevant in the array's visible region. Furthermore, the gain was measured in  $\theta$ -space (2), which means that a conversion to  $\psi$ -space is needed. Given that the distance between the antenna elements is  $1/2\lambda$ , this conversion is defined by:

$$\psi = \pi \sin(\theta) \quad (11)$$

Lastly  $\mathbf{E}$  should be normalized to 0 dB for convenience. The element factor can then be included in (5) as follows:

$$GE(\psi) = G(\psi) + E(\psi) \quad (12)$$

However, a closed form expression  $E(\psi)$  for the element factor is not available, only a set of measurements  $\mathbf{E}$ . One could evaluate  $G(\psi)$  at the same angles as  $\mathbf{E}$  and obtain a numerical representation of (12), however, there are some downsides to this approach. Firstly, the synthesis algorithm relies on finding local extrema which requires a certain 'smoothness' that a numerical representation does not exhibit. Secondly, when a

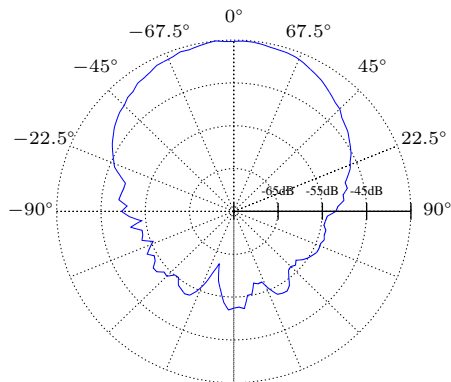


Fig. 3. Measured antenna gain

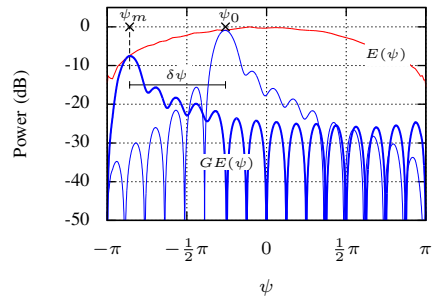


Fig. 4. Beam pattern (shifted) using non-isotropic antennas.

very small ripple is desired (e.g.,  $\leq 0.1$  dB, the minima and maxima eventually become so small that they are difficult to detect using numerical methods. In most cases polynomial fitting can be applied to  $\mathbf{E}$  to obtain an expression  $E(\psi)$  for the element factor. The extrema can then be found algebraically which is more robust.

### C. Element factor alignment

The result of including the element factor can be seen in Fig. 4. Unlike the array factor  $G(\psi)$ , the beam pattern's shape  $GE(\psi)$  is clearly affected when it is shifted, if the array consists of non-isotropic antennas. During synthesis,  $\psi_m$  must therefore always remain aligned with  $\psi_0$  to obtain excitations that compensate the element factor correctly. Such an alignment can be achieved by either shifting  $E(\psi)$  along with  $S(\psi)$ , or by shifting  $G(\psi)$  such that  $\psi_m = \psi_0$  always holds. When the fixed root is at  $-\pi$ , as suggested in section III-A,  $G(\psi)$  itself is also more or less fixed. Because of this and the fact that the latter alternative was found to be cumbersome, alignment of  $E(\psi)$  will be explained in more detail.

$G(\psi)$  is a periodic function with a period of  $2\pi$ , which means that it repeats itself outside the visible region [11]. Effectively this causes  $G(\psi)$  to wrap itself around  $-\pi/\pi$  when it is shifted. Due to this property and because only the visible region is of interest,  $E(\psi)$  may also be wrapped around the visible region in the direction of  $\delta\psi$ :

$$E'(\psi) = E(\psi - \delta\psi + \pi) \bmod 2\pi \quad (13)$$

for synthesis purposes (Fig. 5). Substituting  $E'(\psi)$  for  $E(\psi)$  in (12) yields an expression in which the element and array factor are correctly aligned. It should be noted that  $\psi_m$  may change slightly after displacing the roots of  $G(\psi)$ . This means that  $\delta\psi$  needs to be recalculated and  $E(\psi)$  realigned for each synthesis iteration. It is also important to realize that the direction of  $\delta\psi$  changes when  $\psi_0 < \psi_m$ .

### D. Piecewise approximation

The shifted version  $\mathbf{E}'$  of the measured antenna gain can often not be approximated properly by a polynomial. Wrapping the element factor introduces discontinuity (Fig. 5), or at least a sudden jump, at  $\psi_p$ :

$$\psi_p = \begin{cases} \pi + \delta\psi, & \delta\psi < 0 \\ -\pi - \delta\psi, & \delta\psi > 0 \end{cases} \quad (14)$$

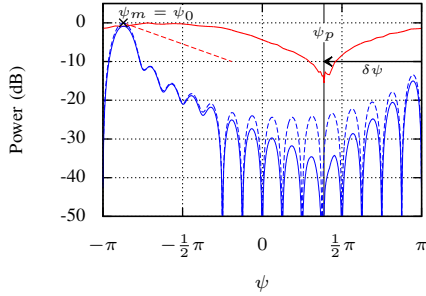


Fig. 5. Element factor alignment.

The approximation suffers considerably from this discontinuity as can be seen in Fig. 6(a). Much better results are obtained when  $E'(\psi)$  is fitted piecewise from  $-\pi$  to  $\psi_p$ , and from  $\psi_p$  to  $\pi$ , as illustrated in Fig. 6(b).

Let  $E_l(\psi)$  be the curve fitted to the data points from  $\mathbf{E}'$ , where  $\psi \leq \psi_p$ , and  $E_r(\psi)$  the curve fitted to the data from  $\psi > \psi_p$ . The expression for the beam pattern, including the aligned element factor, then becomes:

$$GE(\psi) = \begin{cases} G(\psi) + E_l(\psi), & \psi \leq \psi_m \\ G(\psi) + E_r(\psi), & \psi > \psi_m \end{cases} \quad (15)$$

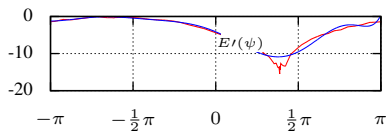
Using this expression for synthesis will yield a beam pattern which does not suffer from the non-uniform gain of the physical antennas used in the array.

#### IV. APPLICATION TO A RAMP SHAPED PATTERN

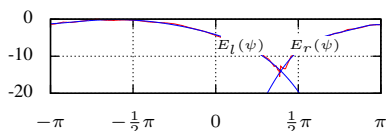
To demonstrate the effectiveness of the proposed modifications, the result of synthesizing the ramp shaped pattern with a maximum ripple of 0.1 dB is shown. The desired shape (Fig. 7) is defined as:

$$S_r(\theta) = \begin{cases} -30 \text{ dB}, & \theta < -45^\circ \\ -(1/4 \times \theta) - 5 \text{ dB}, & -45^\circ \leq \theta \leq 5^\circ \\ -30 \text{ dB}, & -5^\circ < \theta \end{cases} \quad (16)$$

Region I ( $-45^\circ \dots -5^\circ$ ) is intentionally chosen close to endfire, where the non-uniformity of the antenna gain is most notable.



(a) 26<sup>th</sup> order curve fitting



(b) 5<sup>th</sup> order piecewise fitted curves

Fig. 6. Shifted element factor approximation.

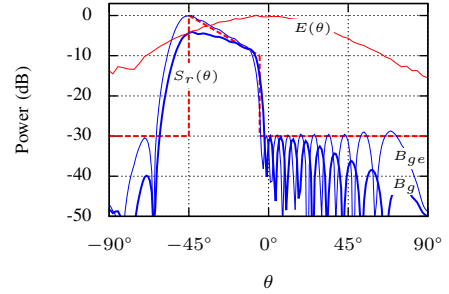


Fig. 7. Shaped pattern synthesis with ( $B_{ge}$ ) and without ( $B_g$ ) compensation.

The pattern resulting from standard Orchard Elliott synthesis is plotted as the thick line in Fig. 7. Note that the power is almost 5 dB below the specification at  $\theta = -45^\circ$ . Such a large difference will lead to a large error in the DoA estimated by the method in [7]. Using the proposed modifications, the pattern's shape is much closer to specification, as illustrated by the thin line. The small deviations in the sidelobe height are caused by the polynomial approximation.

#### V. COMPUTATIONAL STABILITY

Finding the local maxima in region II can be problematic when  $\psi_p$  coincides with one of the lobes. The sudden jump of  $E(\psi)$  at angle  $\psi_p$  causes the appearance of two small peaks in  $GE(\psi)$ , as depicted in Fig. 8. This is problematic because the algorithm expects exactly  $N_2$  maxima while  $N_2 + 1$  maxima are found. Let  $w_l$  be the first root to the left of  $\psi_p$  and  $w_r$  the first root to the right of  $\psi_p$  (Fig. 8). To solve the issue, one could interpolate the expected  $GE(\psi)$  curve between  $w_l$  and  $w_r$ . However, this requires a fair amount of computation while for most applications a satisfactory single peak location, say  $\psi_r$ , can be found using  $G(\psi)$  on that interval. Depending on whether  $\psi_r < \psi_p$  or  $\psi_r > \psi_p$ ,  $G(\psi_r) + E_l(\psi_r)$  or  $G(\psi_r) + E_r(\psi_r)$  will give the desired height of the lobe. A similar repair would be extremely hard for region I. Shaping patterns where  $\psi_0 < \psi_p < \psi_1$  (i.e., shapes defined across the visible region's ends) are therefore best avoided.

A different problem may arise when  $\psi_0$  and  $\psi_m$  are close together. When  $\psi_p$  ends up too close to  $-\pi$  or  $\pi$ , there will be insufficient data points to fit  $E_l(\psi)$  or  $E_r(\psi)$  uniquely. When this is the case,  $GE(\psi)$  should be replaced by either  $G(\psi) + E_l(\psi)$  or  $G(\psi) + E_r(\psi)$ , for all  $\psi$ . At which distance between  $\psi_0$  and  $\psi_m$  this measure is needed depends on how fine grained  $E(\theta)$  was measured. As a rule of thumb it can be said that when  $\psi_p < \psi_m$ , it is better to use  $G(\psi) + E_r(\psi)$  instead of (14), and  $G(\psi) + E_l(\psi)$  when  $\psi_m$  is to the right of the right-most peak in  $G(\psi)$ .

#### VI. DISCUSSION

There are some downsides to element factor aware synthesis. Firstly one can (generally) expect longer computation times. These result mainly from the additional calculations required for the  $GE(\psi)$  expression. However, the convergence rate now also varies with the positioning of region I. Convergence rates of synthesizing the ramp, flat-top and  $\text{csc}^2(\theta) \times \cos(\theta)$  shaped patterns, with a maximum ripple of 0.1 dB, can be found in Table I. The second column represents

TABLE I  
SYNTHESIS CONVERGENCE (# ITERATIONS)

	$G$	$GE$ -60°...-20°	$GE$ -40°...0°	$GE$ -20°...20°	$GE$ 0°...40°	$GE$ 20°...60°
flat	5	6	6	6	6	6
ramp	6	12	11	13	22	14
$\text{csc}^2(\theta) \times \cos(\theta)$	13	6	11	13	14	14

conventional Orchard Elliott ( $G$ ) synthesis and columns three to seven list element factor synthesis ( $GE$ ) for different locations of region I. In most cases element factor compensation results in slower convergence, however, occasionally the element factor appears to be beneficial for the converge rate. The additional computation time per iteration varies between 40% and 45%. It should also be noted that synthesizing shaped patterns for a specific element factor means that a pattern needs to be resynthesized when the location of region I is changed. Unlike the array factor, the beam pattern will be affected by rotating all roots simultaneously, as explained in section III-C. Lastly, an increased complexity in the excitations  $I_n$  is likely, as already pointed out in [12]. One should in particular be aware of a higher amplitude range (i.e.,  $\max(|I_n|)/\min(|I_n|)$ ), which requires additional design effort with respect to mutual coupling.

## VII. CONCLUSION

The Orchard Elliott synthesis method is an attractive option when shaped beam patterns need to be designed for equispaced linear arrays, with high precision. A modification of this algorithm has been presented, which takes the element factor into account. The modification compensates for the directivity of antenna elements, which is particularly of interest for patterns that have their shaped region outside the broadside area. Synthesis of various shaped patterns, compensated for a realistic element factor, has been evaluated successfully using the proposed method. Still achieving a 0.1 dB ripple, this indicates that the proposed modification has no negative effect on the precision. It does entail increased computation time, however, the strength of the Orchard Elliott method is its excellent control over the pattern's shape rather than delivering results fast. In addition, it can be said that shaping beam patterns is predominantly a task that is performed offline. The additional computation time should therefore not be a major drawback.

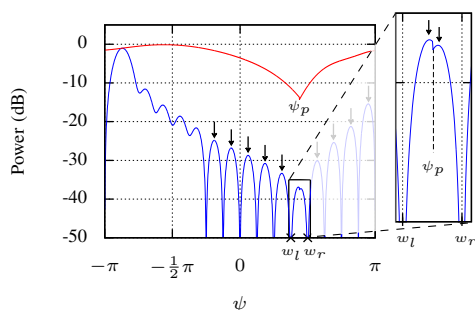


Fig. 8. Problems with peak detection due to element factor alignment.

## ACKNOWLEDGMENT

This work is part of the SOWICI research project (647.000.005), which is financed by the Netherlands Organization for Scientific Research. The authors would like to thank Zizheng Cao from the University of Technology in Eindhoven for measuring the antenna gain.

## REFERENCES

- [1] P. M. Woodward, "A method of calculating the field over a plane aperture required to produce a given polar diagram," *Journal of the Institution of Electrical Engineers - Part IIIA: Radiolocation*, vol. 93, no. 10, pp. 1554–1558, September 1946.
- [2] J. A. Ferreira and F. Ares, "Pattern synthesis of conformal arrays by the simulated annealing technique," *Electronics Letters*, vol. 33, no. 14, pp. 1187–1189, July 1997.
- [3] F. J. Ares-Pena, J. A. Rodriguez-Gonzalez, E. Villanueva-Lopez, and S. R. Rengarajan, "Genetic algorithms in the design and optimization of antenna array patterns," *IEEE Transactions on Antennas and Propagation*, vol. 47, no. 3, pp. 506–510, March 1999.
- [4] D. Gies and Y. Rahmat-Samii, "Particle swarm optimization for reconfigurable phase-differentiated array design," *Microwave and Optical Technology Letters*, vol. 38, no. 3, pp. 168–175, January 2003.
- [5] L. I. Vaskelainen, "Constrained least-squares optimization in conformal array antenna synthesis," *IEEE Transactions on Antennas and Propagation*, vol. 55, no. 3, pp. 859–867, March 2007.
- [6] B. Fuchs, "Shaped beam synthesis of arbitrary arrays via linear programming," *IEEE Antennas and Wireless Propagation Letters*, vol. 9, pp. 481–484, June 2010.
- [7] T. Buintjes, A. Kokkeler, G. Karagiannis, and G. Smit, "Using shaped beam patterns for tracking," *IEEE Transactions on Antennas and Propagation*, vol. 62, no. 12, pp. 6496–6501, December 2014.
- [8] H. J. Orchard, R. S. Elliott, and G. J. Stern, "Optimising the synthesis of shaped beam antenna patterns," *IEEE Proceedings of Microwaves, Antennas and Propagation*, vol. 132, no. 1, pp. 63–68, February 1985.
- [9] S. A. Schelkunoff, "A mathematical theory of linear arrays," *Bell System Technical Journal*, vol. 22, no. 1, pp. 80–107, Januari 1943.
- [10] R. S. Elliott and G. J. Stern, "A new technique for shaped beam synthesis of equispaced arrays," *IEEE Transactions on Antennas and Propagation*, vol. 32, no. 10, pp. 1129–1133, October 1984.
- [11] H. L. van Trees, *Optimum Array Processing (Detection, Estimation, and Modulation Theory, Part IV)*, 1st ed. Wiley-Interscience, March 2002, ch. 2&3.
- [12] F. Ares-Pena, "A note on the limitations of orchard's method," *IEEE Antennas and Propagation Magazine*, February 2002.
- [13] R. S. Elliott, "Improved pattern synthesis for equispaced linear arrays," *Alta Frequenza rivista di radiotecnica, telefonia e acustica applicata*, vol. 51, no. 1, pp. 296–300, November 1982.
- [14] Z. Cao, Q. Wang, R. Lu, A. C. F. Reniers, H. P. A. van den Boom, E. Tangdionga, and A. M. J. Koonen, "Microwave beam steering with tunable spectral filtering using cyclic additional optical true time delay," in *Optical Fiber Communication*, March 2014.